observed in these studies suggests that there are no major structural or electronic differences between F430 and F430M in TFE-$d_3$ and $CD_2Cl_2$ solutions, respectively. Qualitative analyses of the 2D NOESY data are consistent with stereochemical assignments made previously for F430M with 1D NOE methods and are also consistent with an *R* stereochemistry assignment for the C17 carbon. However, additional experiments will be necessary to establish unambiguously whether the C17–C18–C19 stereochemical assignments are *R,R,S* or *S,S,R*, respectively. Although the $^1H$ NMR signals exhibited by native F430 are relatively broad even at 500-MHz field strength, it is clearly possible to obtain detailed structural information and signal assignments from small sample quantities (2 mg) with the recently developed 2D NMR experiments. Having confirmed aspects of the covalent structure and completed the $^1H$ NMR assignment, we have set the stage for determination of the 3D solution structure of native F430 to atomic level resolution using new 2D NOESY back-calculation and distance geometry methods (underway).

**Acknowledgment.** Financial support from the Petroleum Research Fund, administered by the American Chemical Society (to M.F.S.), and the NSF (Grant 1-5-29812 NSF DMB 86-13679 to R.W.) and technical support from Victor Gabriel (UIUC), Scott Smith (UIUC), and Jack Suess (UMBC) are gratefully acknowledged.

**Registry No.** Coenzyme F430, 73145-13-8.

**Supplementary Material Available:** Expansions of 2D HOHAHA spectra with labeled *J*-networks (Figure S1), 2D HOHAHA spectra at low contour levels (Figure S2), full 2D $^1H$–$^{13}C$ HMQC spectrum of F430 (Figure S3), portions of 2D HMBC spectrum for F430 (Figures S4 and S5), and UV–vis spectra of F430 in $H_2O$ and TFE-$d_3$ (Figure S6) (6 pages). Ordering information is given on any current masthead page.

# Infrared Intensities: Bicyclo[1.1.0]butane. A Normal Coordinate Analysis and Comparison with Cyclopropane and [1.1.1]Propellane

**Kenneth B. Wiberg,* Sherman T. Waddell, and Robert E. Rosenberg**

*Contribution from the Department of Chemistry, Yale University, New Haven, Connecticut 06511.*
*Received June 16, 1989*

**Abstract:** The infrared and Raman spectra of bicyclo[1.1.0]butane and of its *1,3-$d_2$* and *2,2,4,4-$d_4$* isotopomers were redetermined, and the intensities of the infrared bands were measured. A new vibrational assignment was made with the help of the spectrum calculated by using the 6-31G* basis set. A normal coordinate analysis was carried out, and the infrared intensities were converted to atomic polar tensors and to dipole moment derivatives with respect to symmetry coordinates. The results of this investigation are compared with the data for cyclopropane and for [1.1.1]propellane in order to determine the effect of the structural changes on the properties of the methylene groups of these molecules.

## I. Introduction

One of the goals of physical organic chemistry is to be able to describe structural and substituent effects in as detailed a fashion as possible. Molecular spectroscopy has the potential for providing such information. As an example, consider the methylene groups of cyclopropane (**1**), bicyclo[1.1.0]butane (**2**), and [1.1.1]propellane (**3**). If it were possible to determine the force constants for the vibrations of the methylene groups, along with the dipole moment derivatives for these vibrations, one would have a good description of how the group changes through the series.

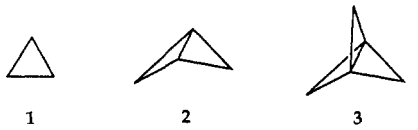

1 2 3

We have presented a normal coordinate analysis for [1.1.1]propellane and have determined the dipole moment derivatives with respect to the symmetry coordinates.[1] Corresponding data for cyclopropane also are available.[2] We have reported a vibrational assignment and a normal coordinate analysis for bicyclobutane,[3] and another assignment has been reported by Aleksanyan et al.[4] However, they must be considered as first approximations since many of the bands are quite weak and relatively difficult to assign. In addition, it now seems clear that a unique force field cannot be obtained for a polyatomic molecule by using only observed vibrational frequencies.[5] The off-diagonal elements of the force constant matrix are often coupled to the diagonal terms so that changes in one may be compensated by changes in the other without significantly changing the calculated frequencies. Therefore, we have reinvestigated the vibrational spectrum of **2** with the aid of theoretical calculations, and in addition, we have measured the intensities of the infrared bands so that the changes in dipole moment resulting from molecular distortions could be determined.

## II. Vibrational Spectrum of Bicyclobutane

The two main problems with bicyclobutane are those of making a satisfactory vibrational assignment for the weaker bands in the spectrum and of finding a unique solution to the normal coordinate problem. A calculation of the vibrational spectrum with ab initio MO theory provides useful information.[6] First, after appropriate scaling, the calculated frequencies and intensities are a good guide to what should be found for each symmetry block.[7] Second, the

(1) Wiberg, K. B.; Dailey, W. P.; Walker, F. H.; Waddell, S. T.; Crocker, L. S.; Newton, M. D.; *J. Am. Chem. Soc.* **1985**, *107*, 7247.
(2) Kondo, S.; Nakanaga, T.; Saëki, S. *Spectrochim. Acta* **1979**, *35A*, 181.
(3) Wiberg, K. B.; Peters, K. S. *Spectrochim. Acta* **1977**, *33A*, 261.
(4) Aleksanyan, V. T.; Ezernitskaya, M. G.; Zotova, S. V.; Abramova, N. M. *Izv. Akad. Nauk. SSSR, Ser. Khim.* **1976**, *1*, 81.
(5) For an extreme example of multiple force fields see: Wiberg, K. B.; Dempsey, R. C.; Wendoloski, J. J. *J. Phys. Chem.* **1984**, *88*, 5596.
(6) Hess, B. A., Jr.; Schaad, L. J.; Carsky, P.; Zahradnik, R. *Chem. Rev.* **1986**, *86*, 709.

0002-7863/90/1512-2184$02.50/0 

**Table I.** Comparison of Observed and Calculated Structures for Bicyclobutane

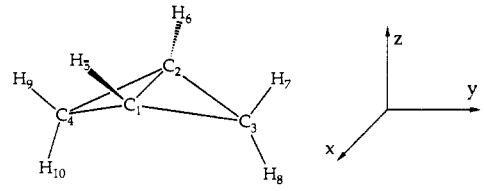


| parameter | obsd | calcd |
|---|---|---|
| | Distances, Å | |
| $r(C_1-C_2)$ | 1.497 ± 0.003 | 1.466 |
| $r(C_1-C_3)$ | 1.498 ± 0.004 | 1.489 |
| $r(C_1-H_5)$ | 1.071 ± 0.004 | 1.071 |
| $r(C_3-H_7)$ | 1.093 ± 0.008 | 1.078 |
| $r(C_1-H_8)$ | 1.093 ± 0.008 | 1.082 |
| | Angles, deg | |
| $\angle C_1-C_2-H_6$ | 128.4 ± 0.2 | 131.4 |
| ∠H-C-H | 115.6 | 114.0 |
| $\angle C_1-C_3-C_2$ | 60.0 | 59.0 |
| $\angle C_3-C_1-H_5$ | 130.4 | 130.5 |
| ∠C3-c-C4[a] | 122.7 ± 0.5 | 120.6 |
| ∠c-C3H7 | 122.9 ± 0.8 | 121.4 |
| ∠c-C3-H8 | 121.6 ± 0.9 | 124.7 |

[a] c is the center of the bridgehead C-C bond.

**Table II.** Calculated and Assigned Vibrational Frequencies for Bicyclobutane[a]

| mode | | calcd | scaled | calcd intensity IR | calcd intensity Raman | dep. ratio | assignments ref 3 | assignments ref 4 |
|---|---|---|---|---|---|---|---|---|
| $A_1$ | 1 | 3437 | 3128 | 3.9 | 117.5 | 0.06 | 3122 | 3129 |
| | 2 | 3343 | 3042 | 33.7 | 103.5 | 0.62 | 2925 | 3038 |
| | 3 | 3251 | 2958 | 62.9 | 195.1 | 0.16 | 2896 | 2933 |
| | 4 | 1684 | 1482 | 0.01 | 8.5 | 0.62 | 1302 | 1493 |
| | 5 | 1417 | 1247 | 1.27 | 31.2 | 0.01 | 1264 | 1261 |
| | 6 | 1210 | 1065 | 0.01 | 13.7 | 0.23 | 1242 | 1240 |
| | 7 | 958 | 843 | 0.51 | 17.3 | 0.73 | 1080 | 1088 |
| | 8 | 802 | 706 | 9.02 | 3.0 | 0.57 | 658 | 648 |
| | 9 | 473 | 416 | 1.01 | 1.5 | 0.32 | 422 | 422 |
| $A_2$ | 10 | 1306 | 1149 | 0.0 | 0.22 | 0.75 | 1140 | 1159 |
| | 11 | 1205 | 1060 | 0.0 | 0.43 | 0.75 | 1090 | 1078 |
| | 12 | 1010 | 889 | 0.0 | 22.3 | 0.75 | 912 | 908 |
| | 13 | 935 | 823 | 0.0 | 1.8 | 0.75 | 650 | |
| $B_1$ | 14 | 3423 | 3115 | 8.2 | 73.6 | 0.75 | 2949 | 3117 |
| | 15 | 1305 | 1148 | 14.4 | 9.4 | 0.75 | 1268 | 1108 |
| | 16 | 1248 | 1098 | 2.4 | 11.7 | 0.75 | 1113 | 980 |
| | 17 | 1133 | 997 | 4.6 | 0.2 | 0.75 | 983 | 838 |
| | 18 | 825 | 726 | 78.3 | 0.7 | 0.75 | 735 | 735 |
| $B_2$ | 19 | 3345 | 3044 | 23.0 | 56.7 | 0.75 | 3044 | 3042 |
| | 20 | 3251 | 2958 | 51.2 | 5.0 | 0.75 | 2971 | 2967 |
| | 21 | 1644 | 1447 | 1.1 | 8.1 | 0.75 | 1456 | 1448 |
| | 22 | 1445 | 1272 | 1.5 | 1.7 | 0.75 | 1149 | 1376 |
| | 23 | 1192 | 1049 | 0.8 | 10.2 | 0.75 | 940 | 1143 |
| | 24 | 1034 | 910 | 0.9 | 0.4 | 0.75 | 851 | 930 |

[a] The band positions are given in $cm^{-1}$, the infrared intensities are given in km/mol, the Raman intensities are given in $\alpha^4$/amu, and dep. ratio is the calculated Raman depolarization ratio.

calculated force constants, after similar scaling, provide a useful starting point for a normal coordinate calculation. The calculated force constants provide good estimates of the off-diagonal terms which are not readily determined in other ways. The use of the same level of theory for a group of related compounds should ensure that consistent results are obtained.

The vibrational spectrum was calculated with use of the 6-31G* basis set at the calculated equilibrium geometry (Table I). As usual, the bond lengths[8] were too short by ~1-2%, which leads to calculated force constants that are somewhat too large.[9] In addition, the calculated modes are harmonic, whereas the observed modes are anharmonic and generally have lower vibrational frequencies. In other studies, we found that the calculated frequencies for the C-H stretching modes should be scaled by 0.91 and those for the other modes by 0.88.[10] This usually leads to an root-mean-square deviation between scaled and observed frequencies of about 25 $cm^{-1}$. The scaled calculated vibrational frequencies are compared with the previous vibrational assignments in Table II. It can be seen that there are a number of points of disagreement between the earlier assignments, as well as between the calculated spectrum and the assignments.

It appeared desirable to reexamine the experimental data in order to obtain a more satisfactory vibrational assignment. Survey IR and liquid-phase Raman spectra are available in our earlier study of bicyclobutane.[3] The use of an FT-IR spectrometer would permit the band shapes to be more carefully examined, and a resolution of 0.06 $cm^{-1}$ was employed with a Nicolet 7199 spec-

**Table III.** Gas-Phase Vibrational Frequencies for Bicyclobutane

| infrared spectrum freq, $cm^{-1}$ | rel int | assignment | Raman spectrum freq, $cm^{-1}$ | rel int | assignment |
|---|---|---|---|---|---|
| 3131.2 | w | $\nu_1$ | 3133 | s | $\nu_1$ |
| 3119.7 | w | $\nu_{14}$ | 3047 | m | $\nu_{19}$ |
| 3043.7 | s | $\nu_2$, $\nu_{19}$ | 3043 | m | $\nu_2$ |
| 2968.7 | s | $\nu_{20}$ | 2968 | w | $\nu_{20}$ |
| 2935.4 | s | $\nu_3$ | 2937 | s | $\nu_3$ |
| 2902 | s | $2\nu_{21}$? | 2889 | s | $\nu_4 + \nu_5$? |
| 2888 | s | $\nu_4 + \nu_5$? | 1501 | w | $\nu_4$ |
| 1630 | w | $\nu_8 + \nu_{17}$ | 1485 | w | $\nu_{21}$ |
| 1484.6 | w | $\nu_{21}$ | 1453 | w | $2\nu_{18}$ |
| 1453 | w | $2\nu_{18}$ | 1315 | m | $\nu_9 + \nu_{12}$ |
| 1394 | w | $\nu_8 + \nu_{18}$ | 1295 | m | $2\nu_8$ |
| 1295 | w | $2\nu_8$ | 1266 | s | $\nu_5$ |
| 1266.0 | m | $\nu_5$, $\nu_{22}$ | 1245 | s | $\nu_7 + \nu_9$ |
| 1245 | w | $\nu_7 + \nu_9$ | 1093 | s | $\nu_{16}$ |
| 1145 | m | $\nu_9 + \nu_{18}$ | 1081 | s | $\nu_6$, $\nu_{23}$ |
| 1110.0 | s | $\nu_{15}$ | 909 | s | $\nu_{12}$ |
| 979.9 | m | $\nu_{17}$ | 859 | w | $2\nu_9$ |
| 935.2 | w | $\nu_{24}$ | 837 | w | $\nu_7$, $\nu_{13}$ |
| 838.8 | w | $\nu_7$ | 658 | m | $\nu_8$ |
| 736.7 | s | $\nu_{18}$ | 422 | m | $\nu_9$ |
| 656.9 | m | $\nu_8$ | | | |
| 422.5 | w | $\nu_9$ | | | |

**Table IV.** Gas-Phase Vibrational Frequencies for Bicyclobutane-$d_2$

| infrared spectrum freq, $cm^{-1}$ | rel int | assignment | Raman spectrum freq, $cm^{-1}$ | rel int | assignment |
|---|---|---|---|---|---|
| 3044.6 | s | $\nu_2$, $\nu_{19}$ | 3044 | m | $\nu_2$, $\nu_{19}$ |
| 2961.9 | s | $\nu_{20}$ | 2977 | m | $2\nu_4$ |
| 2935.0 | s | $\nu_3$ | 2962 | w | $\nu_{20}$ |
| 2889 | w | $\nu_1 + \nu_8$ | 2937 | s | $\nu_3$ |
| 2350 | w | $\nu_1$, $\nu_{14}$ | 2888 | m | $\nu_1 + \nu_8$ |
| 2167 | w | $2\nu_{15}$ | 2350 | s | $\nu_1$, $\nu_{14}$ |
| 1227 | m | $\nu_5$, $\nu_{22}$ | 2180 | w | $\nu_6 + \nu_9$ |
| 1106.7 | s | $\nu_{15}$ | 1490 | w | $\nu_4$ |
| 1020.7 | w | $\nu_{23}$ | 1252 | w | $\nu_7 + \nu_9$ |
| 917 | w | $\nu_8 + \nu_9$ | 1226 | s | $\nu_5$ |
| 827.8 | w | $\nu_7$ | 1186 | w | $\nu_9 + \nu_{17}$ |
| 696.5 | s | $\nu_{18}$ | 1083 | s | $\nu_6$ |
| 510.2 | w | $\nu_8$ | 1078 | w | $\nu_{11}$ |
| | | | 828 | m | $\nu_7$, $\nu_{12}$ |
| | | | 796 | m | $\nu_{17}$ |
| | | | 722 | m | $\nu_{13}$ |
| | | | 511 | m | $\nu_8$ |
| | | | 403 | m | $\nu_9$ |

(7) Pulay, P.; Fogarasi, G.; Pongor, G.; Boggs, J.; Vorgha, A. *J. Am. Chem. Soc.* **1983**, *105*, 7037.
(8) Cox, K. W.; Harmony, M. D.; Nelson, G.; Wiberg, K. B. *J. Chem. Phys.* **1969**, *50*, 1976.
(9) Hehre, W. J.; Radom, L.; Schleyer, P. v. R.; Pople, J. A. *Ab Initio Molecular Orbital Theory*; Wiley: New York, 1986.
(10) Wiberg, K. B.; Walters, V. A.; Colson, S. D. *J. Phys. Chem.* **1984**, *88*, 4723. Wiberg, K. B.; Walters, V. A.; Dailey, W. P. *J. Am. Chem. Soc.* **1985**, *107*, 4860. Wiberg, K. B.; Walters, V. A.; Wong, K.; Colson, S. D. *J. Phys. Chem.* **1984**, *88*, 60067.

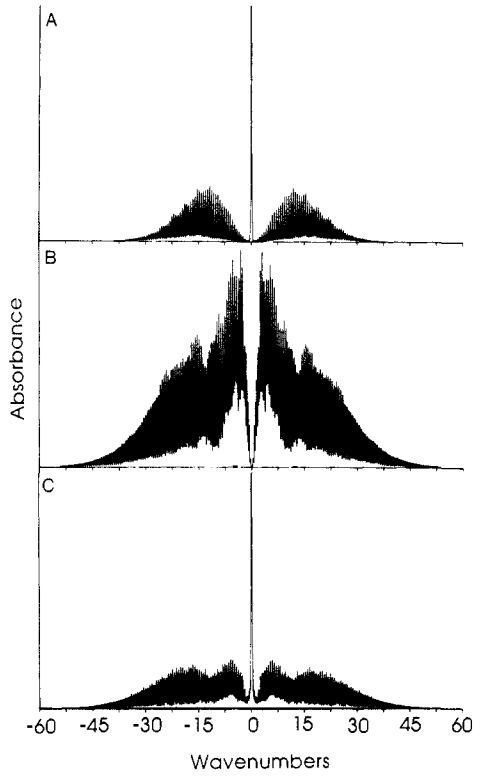


**Figure 1.** Calculated band shapes for bicyclo[1.1.0]butane with use of the ground-state rotational constants. The plots are marked with the band types. The $A_1$ modes give A type bands, the $B_1$ modes give B type bands, and the $B_2$ modes give C type bands.

trometer. The band shapes were simulated[11] (Figure 1) with use of the ground-state rotational constants.[8] In addition, the distortion in the band shapes which would be expected for small changes in the upper state rotational constants were calculated and facilitated the identification of the infrared bands. The earlier Raman data were obtained in the liquid phase. We have now obtained the spectra in the gas phase using a Spex Ramalog spectrometer so that they would be directly comparable with the infrared data. In the gas-phase Raman spectra, the predominant features were the strong Q branches for the $A_1$ vibrations. The spectral data are summarized in Tables III–V for bicyclo-[1.1.0]butane, bicyclobutane-*1,3-d*$_2$, and bicyclobutane-*2,2,4,4-d*$_4$, respectively.

**a. $A_1$ Symmetry Block.** The $A_1$ vibrations may be identified by their strong Q branch in the infrared (Figure 1A) and by their polarized bands in the Raman spectrum. The assignments for $\nu_1$ and $\nu_3$ were easily made since they were expected to give intense and strongly polarized Raman bands. In the case of $\nu_2$, there was a strong Q branch at the expected frequency which appeared to be overlapped with $\nu_{19}$. This band was calculated to have a depolarization ratio of only 0.62. In the parent, there was only one band at ~400 cm$^{-1}$. It was polarized in the Raman spectrum and must be assigned as $\nu_9$. There was only one band, ~650 cm$^{-1}$, that appeared in both the IR and Raman spectra. It must be assigned as $\nu_8$. It was not strongly polarized, but this is consistent with the calculated depolarization ratio of 0.52. Both $\nu_5$ and $\nu_6$ were calculated to be intense in the Raman and weak in the IR. There was a pair of intense polarized bands in the region expected for $\nu_5$, at 1245 and 1266 cm$^{-1}$. The latter value was chosen since it gave a better fit in the normal coordinate analysis. There also was a pair of strong Raman bands in the region expected for $\nu_9$, at 1080 and 1092 cm$^{-1}$. The more strongly polarized band (1080 cm$^{-1}$) was assigned as $\nu_6$. A band appears at 838 cm$^{-1}$ in the Raman, which was reasonably assigned as $\nu_7$. It was not polarized, but that is consistent with the calculated depolarization ratio of 0.73. Finally, the polarized Raman band at 1501 cm$^{-1}$ was assigned as $\nu_4$.

The assignments for $d_2$ and $d_4$ were made in analogy with those for the parent. The details of the assignments are available.[12]

**b. $A_2$ Symmetry Block.** This symmetry block is very difficult to assign because the vibrations are not allowed in the IR, and generally give weak bands in the Raman. The assignment for $\nu_{12}$ (908.6 cm$^{-1}$ for the parent) is secure since it should give a relatively intense Raman band. It is distinctive in giving P and R branches but no Q branch in the gas-phase Raman spectrum. The remaining bands were assigned to the weak feature in the Raman nearest the calculated band positions. These assignments are not very secure.

**c. $B_1$ Symmetry Block.** The infrared bands for this symmetry block have the unique B type contour (Figure 1B) in which the Q branch is absent and the band center appears as the cleft between the P and R branches. This, along with the fact that most of the bands have considerable IR intensity, aids in their identification.

The CH stretching mode of the parent, $\nu_{14}$, was easily identified because of its high frequency, relatively low IR intensity, and unique band shape. There was a very large band in the Raman extending from 3120 to 3140 cm$^{-1}$ which is presumed to result from the overlap of $\nu_1$ and $\nu_{14}$.

The $\nu_{15}$ band was readily identified on the basis of its strong IR band and unique band shape. Nothing was seen in the Raman at ~1100 cm$^{-1}$ despite the prediction of appreciable Raman intensity. The $\nu_{16}$ mode was assigned to a strong Raman band at 1092 cm$^{-1}$. In the gas-phase IR this band was lost in the P branch of $\nu_{15}$, but it could be seen in the liquid-phase IR spectrum. The $\nu_{17}$ mode was assigned to a band at 979.9 cm$^{-1}$ on the basis of its appreciable IR intensity and unique band shape. The $\nu_{18}$ mode was calculated to give the most intense band on the IR spectrum and was found at 736.7 cm$^{-1}$. The assignments for $d_2$ and $d_4$ were made in an analogous fashion.

**d. $B_2$ Symmetry Block.** The infrared bands in this symmetry block have Q branches and appear quite similar to the $A_1$ bands (Figure 1C). The higher frequency CH stretching mode for the parent, $\nu_{19}$, appears to overlap $\nu_2$. The lower frequency CH stretching mode, $\nu_{20}$, was readily observed at 2968.7 cm$^{-1}$. The remaining modes, $\nu_{21}$–$\nu_{24}$, were predicted to give very weak IR bands. The $\nu_{21}$ mode was assigned to a small Raman band at 1484.6 cm$^{-1}$. It was seen as a weak band in the IR with an ambiguous contour. The $\nu_{22}$ mode was expected to be weak in both the IR and Raman spectra and was assigned to a weak IR band with a Q branch at 1261 cm$^{-1}$. The $\nu_{23}$ mode was more

**Table V.** Gas-Phase Vibrational Frequencies for Bicyclobutane-$d_4$

| infrared spectrum | | | Raman spectrum | | |
|---|---|---|---|---|---|
| freq, cm$^{-1}$ | rel int | assignment | freq, cm$^{-1}$ | rel int | assignment |
| 3131.3 | m | $\nu_1$ | 3133 | s | $\nu_1$, $\nu_{14}$ |
| 3119.9 | m | $\nu_{14}$ | 2294 | w | $\nu_2$, $\nu_{19}$ |
| 3043 | | impurity | 2170 | s | $\nu_3$, $\nu_{20}$ |
| 3041 | | impurity | 1310 | s | $\nu_4$ |
| 2957 | m | $\nu_3 + \nu_{24}$ | 1245 | w | $2\nu_{18}$ |
| 2293 | s | $\nu_2$, $\nu_{19}$ | 1059 | m | $\nu_5$ |
| 2155 | s | $\nu_3$, $\nu_{20}$ | 982 | w | $\nu_8 + \nu_9$ |
| 1285.7 | w | $\nu_{22}$ | 959 | w | $\nu_{23}$ |
| 1245 | w | $2\nu_{18}$ | 924 | s | $\nu_6$ |
| 1148 | w | $\nu_7 + \nu_9$ | 898 | w | $\nu_{11}$ |
| 1073.9 | w | $\nu_{15}$ | 824 | m | $\nu_7$ |
| 1059.0 | w | $\nu_5$ | 628 | w | $\nu_8$ |
| 982 | w | $\nu_8 + \nu_9$ | 354 | w | $\nu_9$ |
| 923.9 | w | $\nu_6$ | | | |
| 898.7 | s | $\nu_{17}$ | | | |
| 855.6 | s | $\nu_{16}$ | | | |
| 743.8 | w | $\nu_{24}$ | | | |
| 716 | m | $2\nu_9$ | | | |
| 619.3 | s | $\nu_{18}$ | | | |

(11) The rotational transitions were calculated by using a modification of the XASYROT program of Birss et al. (Birss, F. W.; Colson, S. D.; Ramsay, D. A. *Can. J. Phys.* **1973**, *51*, 1031.)

(12) Waddell, S. T. Ph.D. Thesis, Yale, 1988.

**Table VI.** Vibrational Assignments for Bicyclobutane

| mode | | $d_0$ | $d_2$ | $d_4$ |
|---|---|---|---|---|
| $A_1$ | 1 | 3131.3 | 2354.8 | 3131.3 |
| | 2 | 3043.7 | 3044.6 | 2293.5 |
| | 3 | 2935.0 | 2935.0 | 2157.5 |
| | 4 | 1501.3 | 1490.4 | |
| | 5 | 1266.0 | 1226.8 | 1059.0 |
| | 6 | 1080.7 | 1083.1 | 923.9 |
| | 7 | 838.8 | 827.8 | 824.4 |
| | 8 | 656.9 | 510.2 | 627.5 |
| | 9 | 422.5 | 403.1 | 354.4 |
| $A_2$ | 10 | 1172 | 1124 | |
| | 11 | 1063 | 1078 | 898 |
| | 12 | 908.6 | 722.4 | |
| | 13 | 838 | 827 | |
| $B_1$ | 14 | 3119.7 | 2350 | 3119.9 |
| | 15 | 1110.0 | 1106.7 | 1073.9 |
| | 16 | 1092.0 | 1083.0 | 855.6 |
| | 17 | 979.9 | 795.5 | 898.7 |
| | 18 | 736.7 | 696.5 | 619.3 |
| $B_2$ | 19 | 3043.7 | 3044.6 | 2293.5 |
| | 20 | 2968.7 | 2961.9 | 2155.4 |
| | 21 | 1484.6 | 1478.8 | |
| | 22 | 1261.3 | 1226 | 1285.7 |
| | 23 | 1080.7 | 1020.7 | 959.0 |
| | 24 | 935.2 | 721.1 | 743.8 |

readily assigned since there was a fairly strong Raman band at the expected position, 1080.8 $cm^{-1}$. The $\nu_{24}$ mode was assigned to a weak band with the appropriate contour at 935 $cm^{-1}$.

The assignments for $d_2$ and $d_4$ were made in an analogous fashion. The assignments for all three molecules are summarized in Table VI.

## III. Normal Coordinate Analysis

It has been found for many molecules that there is a good correspondence between the scaled calculated vibrational frequencies and the observed frequencies.[7,10] From this we may conclude that the correspondingly scaled calculated force constants will be good approximations to the force constants needed for a normal coordinate analysis.

The symmetry coordinates chosen for bicyclobutane are summarized in Table VII. This choice leads to no redundant coordinates. The calculated force constants (in Cartesian coordinates) were transformed into those corresponding to the symmetry coordinates by using the appropriate **B** matrix. They were then scaled by a factor of 0.8, which corresponds to the average scaling factor used for the frequencies, and used as a starting point for the normal coordinate analysis. Here, the scaling factors were adjusted to give a "best fit". The diagonal force constants were given independent scaling factors. The problem was constrained by using a single scaling factor for all of the off-diagonal elements for a given symmetry block. The root-mean-square (rms) error for fitting the parent was 7.7 $cm^{-1}$, for $d_2$ it was 10.8 $cm^{-1}$, and for $d_4$ it was 11.6 $cm^{-1}$. The overall rms error was 10.1 $cm^{-1}$. Most of the error was associated with the CH and CD stretching modes. This is expected since these modes are strongly anharmonic, and the anharmonicity corrections are different for CH vs CD.

The results of the normal coordinate analysis are summarized in Table VIII, and the force constants are given in Table IX. The range of scaling factors found in this case was somewhat larger than those we have found in other cases,[10] which might not be surprising for a compound with relatively unusual bonding. The average of the scaling factors was 0.807 ± 0.044, which is a typical value.

The interaction constants were generally fairly small, and there were remarkably few interaction constants greater than 0.25 mdyn/Å. In the $A_1$ block, the larger interaction constants couple the stretching motion of the central C–C bond ($S_9$) with the symmetrical stretching vibration for the other C–C bonds ($S_1$), with the change in the flap angle between the two three-membered rings ($S_2$), and with the C–C–H bending mode for the bridgehead hydrogens ($S_8$). These interactions have already been noted by Gassman and Dixon in another connection.[13] In the $A_2$ block the larger interaction constant was between the C–C stretching motion for the outer C–C bonds ($S_{10}$) and a C–C–H bending mode for the axial C–H bonds ($S_{12}$). A similar large interaction was found between $S_{14}$ and $S_{17}$ in the $B_1$ block.

**Table VII.** Symmetry Coordinates for Bicyclobutane

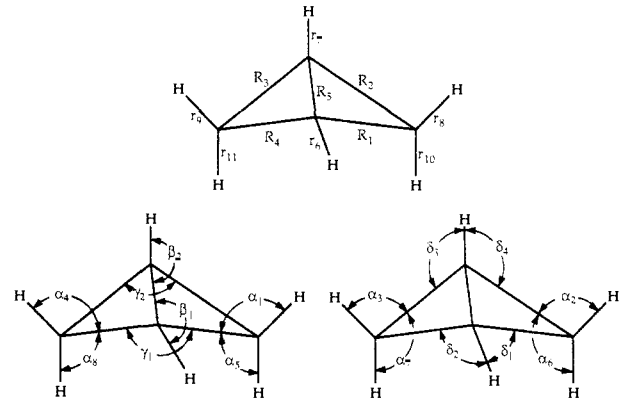

$A_1$
$S_1 = R_1 + R_2 + R_3 + R_4$
$S_2 = \gamma 1 + \gamma 1$
$S_3 = r_6 + r_7$
$S_4 = r_8 + r_9$
$S_5 = r_{10} + r_{11}$
$S_6 = \alpha_1 + \alpha_2 + \alpha_3 + \alpha_4$
$S_7 = \alpha_5 + \alpha_6 + \alpha_7 + \alpha_8$
$S_8 = \beta_1 + \beta_2$
$S_9 = R_5$

$A_2$
$S_{10} = R_1 - R_2 + R_3 - R_4$
$S_{11} = \alpha_1 - \alpha_2 + \alpha_3 - \alpha_4$
$S_{12} = \alpha_5 - \alpha_6 + \alpha_7 - \alpha_8$
$S_{13} = \delta_1 - \delta_2 - \delta_3 + \delta_4$

$B_1$
$S_{14} = R_1 - R_2 - R_3 + R_4$
$S_{15} = r_6 - r_7$
$S_{16} = \alpha_1 - \alpha_2 - \alpha_3 + \alpha_4$
$S_{17} = \alpha_5 - \alpha_6 - \alpha_7 + \alpha_8$
$S_{18} = \beta_1 - \beta_2$

$B_2$
$S_{19} = R_1 + R_2 - R_3 - R_4$
$S_{20} = r_8 - r_9$
$S_{21} = r_{10} - r_{11}$
$S_{22} = \alpha_1 + \alpha_2 - \alpha_3 - \alpha_4$
$S_{23} = \alpha_5 + \alpha_6 - \alpha_7 - \alpha_8$
$S_{24} = \delta_1 - \delta_2 + \delta_3 - \delta_4$

**Table VIII.** Results of Normal Coordinate Analysis

| mode | | $d_0$ obsd | $d_0$ calcd | $d_0$ character[a] | $d_2$ obsd | $d_2$ calcd | $d_4$ obsd | $d_4$ calcd |
|---|---|---|---|---|---|---|---|---|
| $A_1$ | 1 | 3131.2 | 3139 | 80S3 | 2354.8 | 2334 | 3131.3 | 3138 |
| | 2 | 3043.7 | 3051 | 65S4, 23S5 | 3044.6 | 3052 | 2293.5 | 2274 |
| | 3 | 2935.4 | 2942 | 26S4, 67S5 | 2935.0 | 2942 | 2157.5 | 2142 |
| | 4 | 1501.3 | 1502 | 25S1, 29S6, 24S7 | 1490.4 | 1496 | 1310.4 | 1314 |
| | 5 | 1266.0 | 1266 | 34S1, 25S9 | 1226.8 | 1229 | 1059.0 | 1059 |
| | 6 | 1080.7 | 1083 | 32S1 | 1083.1 | 1079 | 923.9 | 919 |
| | 7 | 838.8 | 843 | 36S1, 44S9 | 827.8 | 830 | 824.4 | 809 |
| | 8 | 656.9 | 656 | 33S2, 29S8 | 510.2 | 502 | 627.5 | 631 |
| | 9 | 422.5 | 423 | 40S2, 30S9 | 403.1 | 403 | 354.4 | 357 |
| $A_2$ | 10 | 1172 | 1180 | 21S10, 43S11, 26S12 | 1124 | 1117 | | 1114 |
| | 11 | 1063 | 1084 | 26S11, 61S12 | 1078 | 1068 | 898 | 896 |
| | 12 | 909 | 912 | 43S10, 25S11 | 722 | 713 | | 815 |
| | 13 | 839 | 834 | 70S10 | 827 | 835 | | 653 |
| $B_1$ | 14 | 3119.7 | 3133 | 96S15 | 2350.0 | 2312 | 3119.9 | 3133 |
| | 15 | 1110.0 | 1121 | 41S14, 37S16 | 1106.7 | 1101 | 1073.9 | 1052 |
| | 16 | 1092.0 | 1097 | 30S14, 58S17 | 1083.0 | 1089 | 855.6 | 842 |
| | 17 | 979.9 | 980 | 36S16, 54S18 | 795.5 | 803 | 898.7 | 915 |
| | 18 | 736.7 | 736 | 71S14 | 696.5 | 706 | 619.3 | 606 |
| $B_2$ | 19 | 3043.7 | 3050 | 61S20, 37S21 | 3044.6 | 3050 | 2293.5 | 2274 |
| | 20 | 2968.7 | 2967 | 37S20, 59S21 | 2261.9 | 2967 | 2155.4 | 2156 |
| | 21 | 1484.6 | 1482 | 24S19, 27S22, 41S23 | 1478.8 | 1481 | 1285.7 | 1288 |
| | 22 | 1261.3 | 1263 | 60S19 | 1226.0 | 1225 | | 1079 |
| | 23 | 1080.7 | 1066 | 52S19 | 1020.7 | 1030 | 959.0 | 964 |
| | 24 | 935.2 | 924 | 37S19, 24S22, 23S24 | 721.1 | 728 | 743.8 | 748 |

[a] Percentages of the major symmetry coordinate contributors to the normal mode for the $d_0$ species.

(13) Gassman, P. G.; Greenlee, M. L.; Dixon, D. A.; Richismeier, S.; Gougoutas, J. Z. *J. Am. Chem. Soc.* **1983**, *105*, 5865.

**Table IX.** Force Constants for Bicyclobutane with Symmetry Coordinates

A. Diagonal Force Constants, mdyn/Å

| | f | calcd force constants | scaling factors | adjusted force constants |
|---|---|---|---|---|
| $A_1$ | 1,1 | 5.31 | 0.832 | 4.42 |
| | 2,2 | 2.07 | 0.917 | 1.90 |
| | 3,3 | 6.43 | 0.834 | 5.36 |
| | 4,4 | 6.10 | 0.832 | 5.08 |
| | 5,5 | 5.88 | 0.818 | 4.81 |
| | 6,6 | 0.90 | 0.836 | 0.75 |
| | 7,7 | 0.86 | 0.785 | 0.67 |
| | 8,8 | 0.46 | 0.675 | 0.31 |
| | 9,9 | 5.44 | 0.742 | 4.04 |
| $A_2$ | 10,10 | 4.83 | 0.781 | 3.77 |
| | 11,11 | 1.18 | 0.857 | 1.01 |
| | 12,12 | 1.34 | 0.843 | 1.13 |
| | 13,13 | 0.43 | 0.807 | 0.35 |
| $B_1$ | 14,14 | 5.23 | 0.799 | 4.18 |
| | 15,15 | 6.42 | 0.838 | 5.38 |
| | 16,16 | 1.36 | 0.731 | 0.99 |
| | 17,17 | 1.38 | 0.811 | 1.12 |
| | 18,18 | 0.67 | 0.750 | 0.50 |
| $B_2$ | 19,19 | 5.12 | 0.803 | 4.11 |
| | 20,20 | 6.09 | 0.826 | 5.03 |
| | 21,21 | 5.89 | 0.837 | 4.91 |
| | 22,22 | 0.84 | 0.738 | 0.62 |
| | 23,23 | 0.89 | 0.929 | 0.83 |
| | 24,24 | 0.47 | 0.741 | 0.35 |

B. Off-Diagonal Force Constants

$A_1$ scaling factor = 0.811

| | 2 | 3 | 4 | 5 | 6 | 7 | 8 | 9 |
|---|---|---|---|---|---|---|---|---|
| 1 | −0.05 | 0.00 | 0.13 | 0.25 | 0.14 | 0.10 | −0.15 | −0.46 |
| 2 | | −0.09 | 0.08 | −0.04 | 0.12 | −0.07 | 0.23 | 0.45 |
| 3 | | | 0.01 | −0.01 | 0.00 | 0.00 | −0.02 | 0.06 |
| 4 | | | | 0.05 | 0.01 | −0.12 | −0.01 | −0.12 |
| 5 | | | | | −0.09 | −0.02 | −0.05 | −0.20 |
| 6 | | | | | | 0.33 | 0.01 | 0.03 |
| 7 | | | | | | | −0.03 | 0.10 |
| 8 | | | | | | | | 0.46 |

$A_2$ scaling factor = 0.879 $B_1$ scaling factor = 0.900

| | 11 | 12 | 13 | | 15 | 16 | 17 | 18 |
|---|---|---|---|---|---|---|---|---|
| 10 | 0.25 | 0.45 | 0.25 | 14 | 0.18 | 0.17 | 0.45 | −0.01 |
| 11 | | 0.01 | −0.05 | 15 | | −0.01 | 0.02 | 0.03 |
| 12 | | | 0.09 | 16 | | | 0.00 | 0.04 |
| | | | | 17 | | | | −0.16 |

$B_2$ scaling factor = 0.753

| | 20 | 21 | 22 | 23 | 24 |
|---|---|---|---|---|---|
| 19 | 0.10 | 0.15 | 0.05 | 0.18 | 0.10 |
| 20 | | 0.05 | −0.01 | −0.10 | 0.00 |
| 21 | | | −0.10 | −0.06 | 0.01 |
| 22 | | | | 0.30 | −0.01 |
| 23 | | | | | 0.02 |

The form of the normal coordinates frequently changes significantly on replacing hydrogen by deuterium. The mode mixing is readily calculated by[14]

$$Q_D = L_D^{-1} L_H Q_H$$

where $Q_H$ are the normal coordinates of the unlabeled molecule, $Q_D$ are those for the labeled species, and $L$ and $L^{-1}$ are derived from the normal coordinate analysis. The product $L_D^{-1}L_H$ is given in Table X. It shows, for example, that the 2334-$cm^{-1}$ band for $d_2$ corresponds to the 3131-$cm^{-1}$ band of $d_0$ and that the $A_2$ modes are strongly mixed on deuteration.

## IV. Infrared Intensities

Information on infrared intensities is useful in several contexts. The conversion of the intensities into dipole moment derivatives depends on the normal coordinates, and a satisfactory transformation is possible only if the normal coordinates for the parent and isotopically labeled species are correct. Thus, they serve as a test of the force field which was derived in a normal coordinate analysis. In addition, the dipole moment derivatives are related to the charge distribution in the molecule,[15] and a comparison of the experimental derivatives with the calculated charge distribution provides interesting information.

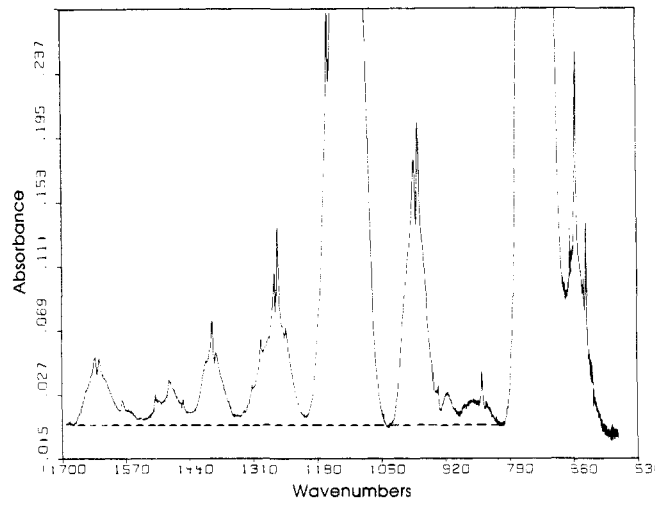


**Figure 2.** The 1700–530 $cm^{-1}$ region for bicyclo[1.1.0]butane at 0.25-$cm^{-1}$ resolution. The lower absorbance region is expanded to show the good linearity of the base line. The base line becomes slightly less satisfactory at ~500 $cm^{-1}$ because of the increased noise level.

The intensities were determined in the gas phase at 0.25-$cm^{-1}$ resolution following the Wilson–Wells–Penner–Weber method.[16] A brass high-pressure cell similar to that described by Dickson et al.[17] with a 72.5 mm path length was used for all measurements. Sample pressures were measured with a Wallace and Tiernan series 300 Bourdon gauge with a rated accuracy of 0.3% of full scale (100 Torr). In our study of cyclopropene[5] it was found that pressure broadening of the rotational lines with 100 psi of nitrogen was adequate to give constant values of measured intensities. With larger moments of inertia, it also should be adequate for bicyclobutane, but to ensure adequate broadening, 300 psi of nitrogen was used. In some cases, the filled cell containing some Teflon chips was shaken, but it had no effect on the observed intensities, indicating that the gases mixed rapidly. The regions chosen for integration were those for which the base line was easily determined. This did not present a problem as can be seen from a portion of the pressure broadened spectrum of the parent in Figure 2. Beer's law plots for the parent compound are shown in Figure 3. The good linearity and zero intercept suggest that the base lines were set satisfactorily. The measured intensity data are summarized in Table XI.

A major problem in dealing with infrared intensities is that of overlapping bands, and the bands which were included in each integration region are noted in Table XI. The CH stretching region (2815–3173 $cm^{-1}$) contains six bands and may readily be partitioned into three regions, each containing two bands (Figure 4). This region is complicated by Fermi resonance of overtones and combination bands with the fundamentals. The assumption was made that the unperturbed intensities for the overtones and combinations was negligible, and each of the three integration regions was divided between the appropriate bands on the basis of the relative calculated intensities. No other procedure was available since both the solution (Figure 4) and liquid-phase spectra were badly overlapped. Although the absolute values of the calculated intensities are in error, it seemed reasonable to use the ratios of the calculated intensities for closely related vibrational

(14) Rava, R. P.; Philis, J. G.; Krogh-Jespersen, K.; Goodman, L. *J. Chem. Phys.* **1983**, *79*, 4664.

(15) Wiberg, K. B.; Wendoloski, J. J. *J. Phys. Chem.* **1984**, *88*, 586.

(16) Wilson, E. B.; Wells, A. *J. Chem. Phys.* **1946**, *14*, 578. Penner, S. S.; Weber, D. *J. Chem. Phys.* **1951**, *19*, 807. Overend, J.; Youngquist, M. J.; Curtis, E. C.; Crawford, B. *J. Chem. Phys.* **1959**, *30*, 532.

(17) Dickson, A. D.; Mills, I. M.; Crawford, B. *J. Chem. Phys.* **1957**, *27*, 445.

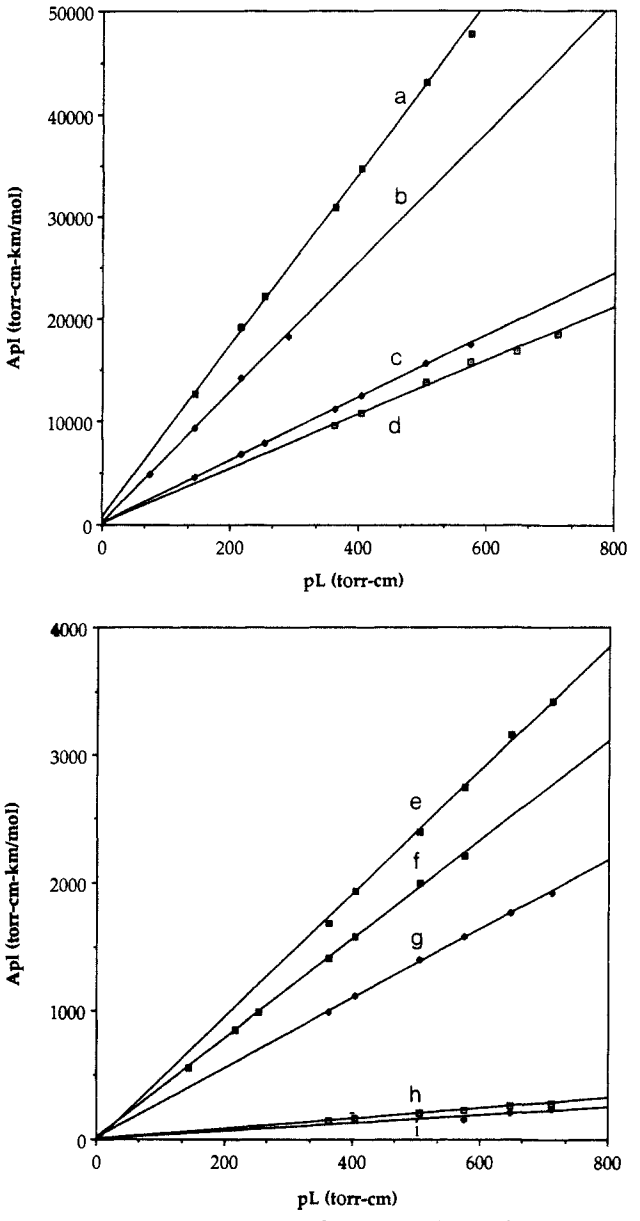


**Figure 3.** (A, top) Beer's law plots for the more intense infrared bands of bicyclo[1.1.0]butane. The integrations ranges were (a) 2825–3007 $cm^{-1}$, (b) 674–802 $cm^{-1}$, (c) 3007–3090 $cm^{-1}$, and (d) 1037–1202 $cm^{-1}$, (B, bottom) Beer's law plots for the less intense bands. The integration regions were (e) 894–1035 $cm^{-1}$, (f) 3093–3173 $cm^{-1}$, (g) 1202–1339 $cm^{-1}$, (h) 1437–1518 $cm^{-1}$, and (i) 803–892 $cm^{-1}$.

modes. It was not possible to find a satisfactory way in which to experimentally partition $\nu_5$ and $\nu_{22}$, and here again we used the ratio of the calculated intensities.

The bands $\nu_{17}$ and $\nu_{24}$ were only partially overlapped, and the integration region was divided into three parts. The first (939–1035 $cm^{-1}$) contained $\nu_{17}$ and the R branch of $\nu_{24}$; the second (930–939 $cm^{-1}$) contained the Q branch of $\nu_{24}$; and the third (894–930 $cm^{-1}$) contained the P branch of $\nu_{24}$. By assuming that the P and R branches of $\nu_{24}$ had equal intensity, the above data allowed the intensities of the two bands to be separated. The region from 1037 to 1202 $cm^{-1}$ was complicated in that it contained one strong fundamental ($\nu_{15}$), two weak fundamentals ($\nu_{16}$ and $\nu_{23}$), and one strong combination ($\nu_9 + \nu_{18}$). The spectrum in $CS_2$ solution (Figure 5) showed a medium band at 1140 $cm^{-1}$ (overtone), a strong band at 1107 $cm^{-1}$ ($\nu_{15}$), and a small band at 1083 $cm^{-1}$ ($\nu_{16}$ and $\nu_{23}$). The spectrum was simulated by using Lorentzian band shapes, allowing the ratio of the areas to be obtained. The gas-phase intensities were separated accordingly, and the band due to $\nu_{16}$ and $\nu_{23}$ was separated on the basis of their calculated intensities.

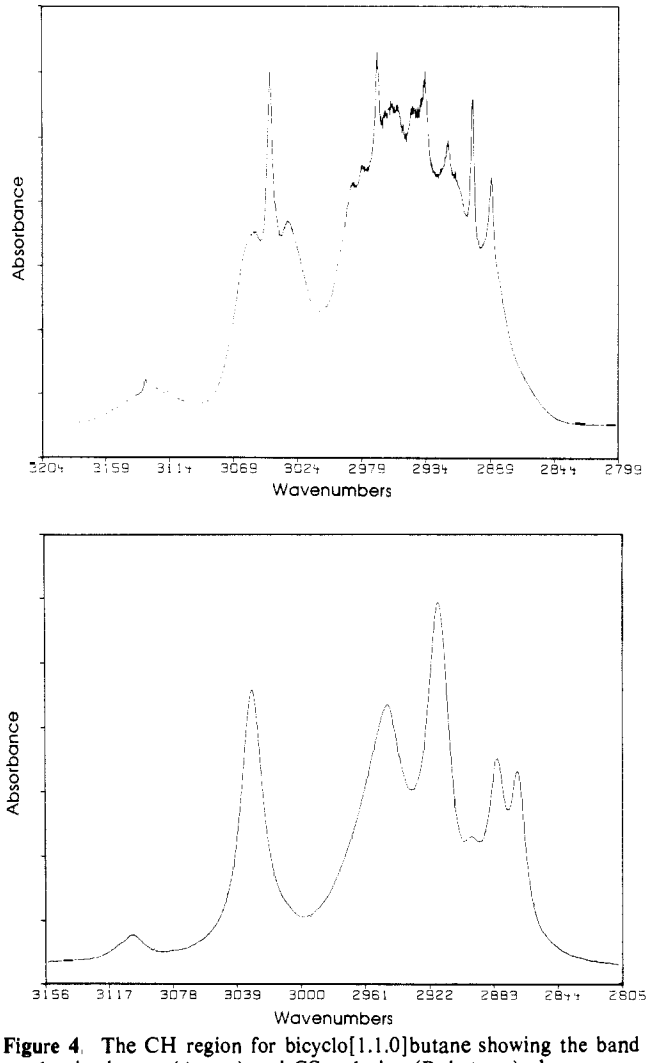


**Figure 4.** The CH region for bicyclo[1.1.0]butane showing the band overlap in the gas (A, top) and $CS_2$ solution (B, bottom) phases.

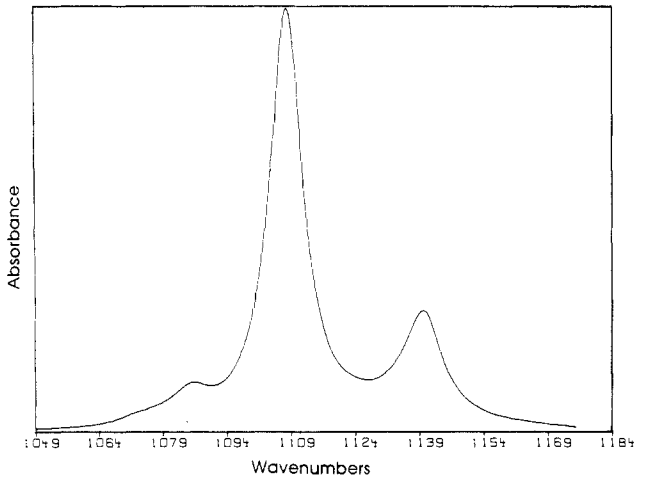


**Figure 5.** The 1049–1184 $cm^{-1}$ region for a $CS_2$ solution of bicyclo-[1.1.0]butane.

The bands for $\nu_4$ and $\nu_6$ were calculated to be weak, were too small to be measured, and were each assigned an intensity of 0.01. The band for $\nu_9$ can be seen in the high-resolution spectrum, but it was obscured by noise in the high-pressure spectrum. It was assigned its calculated intensity.

The intensities assigned to each of the bands are given in Table XII along with the corresponding absolute values of the dipole moment derivatives with respect to the normal coordinates. The latter are compared with the values derived theoretically, and it can be seen that the relative magnitudes are in good agreement.

**Table X.** Normal Modes of Biocyclobutane-$d_2$ and Bicyclobutane-$d_4$

a. Normal Modes of Bicyclobutane-$d_2$, in Terms of Those for Bicyclobutane

| $A_1$ block | normal modes of bicyclobutane | | | | | | | | | $A_2$ block | normal modes of bicyclobutane | | | |
|---|---|---|---|---|---|---|---|---|---|---|---|---|---|---|
| $d_2$, cm$^{-1}$ | 1 | 2 | 3 | 4 | 5 | 6 | 7 | 8 | 9 | $d_2$, cm$^{-1}$ | 10 | 11 | 12 | 13 |
| 3052 | 0.115 | 0.993 | 0.002 | 0.000 | 0.000 | 0.000 | 0.000 | 0.000 | 0.000 | 1117 | −0.887 | 0.460 | −0.215 | 0.008 |
| 2942 | 0.033 | −0.006 | 1.000 | 0.000 | 0.000 | 0.000 | 0.000 | 0.000 | 0.000 | 1068 | 0.441 | 0.881 | 0.250 | −0.009 |
| 2334 | 1.325 | −0.145 | −0.040 | 0.039 | −0.060 | 0.006 | 0.003 | 0.001 | 0.002 | 835 | −0.026 | −0.100 | 0.094 | 0.996 |
| 1496 | −0.112 | 0.012 | 0.003 | 1.001 | 0.053 | −0.003 | −0.002 | 0.000 | −0.001 | 713 | 0.609 | 0.213 | −1.169 | 0.102 |
| 1229 | 0.286 | −0.029 | −0.007 | −0.068 | 1.022 | 0.021 | 0.004 | 0.007 | 0.003 | | | | | |
| 1079 | −0.042 | 0.005 | 0.002 | 0.007 | −0.026 | 1.002 | −0.027 | 0.027 | 0.003 | | | | | |
| 830 | −0.042 | 0.005 | 0.002 | 0.005 | −0.011 | 0.034 | 0.999 | 0.140 | −0.009 | | | | | |
| 502 | −0.034 | 0.002 | −0.003 | 0.004 | −0.033 | −0.093 | −0.262 | 1.190 | 0.323 | | | | | |
| 403 | 0.080 | −0.009 | −0.005 | −0.008 | 0.005 | −0.069 | −0.173 | 0.604 | −0.979 | | | | | |

| $B_1$ block | normal modes of bicyclobutane | | | | | $B_2$ block | normal modes of bicyclobutane | | | | | |
|---|---|---|---|---|---|---|---|---|---|---|---|---|
| $d_2$, cm$^{-1}$ | 14 | 15 | 16 | 17 | 18 | $d_2$, cm$^{-1}$ | 19 | 20 | 21 | 21 | 23 | 24 |
| 2312 | 1.351 | 0.029 | −0.018 | −0.005 | −0.012 | 3050 | −1.000 | 0.000 | 0.000 | 0.000 | 0.000 | 0.000 |
| 1101 | −0.123 | 0.951 | 0.265 | 0.209 | 0.005 | 2967 | 0.000 | 1.000 | 0.000 | 0.000 | 0.000 | 0.000 |
| 1089 | 0.148 | −0.286 | 0.966 | 0.027 | −0.020 | 1481 | 0.000 | 0.000 | 1.000 | −0.023 | −0.010 | −0.009 |
| 803 | −0.132 | 0.287 | 0.106 | −1.101 | −0.340 | 1225 | 0.001 | 0.000 | −0.025 | −0.990 | 0.197 | 0.121 |
| 706 | 0.121 | 0.108 | 0.091 | −0.502 | 0.967 | 1030 | −0.001 | 0.000 | 0.015 | 0.173 | 0.929 | −0.376 |
| | | | | | | 728 | −0.004 | −0.001 | 0.048 | 0.412 | 0.556 | 1.135 |

b. Normal Modes of Bicyclobutane-$d_4$ in Terms of Those for Bicyclobutane

| $A_1$ block | normal modes of bicyclobutane | | | | | | | | | $A_2$ block | normal modes of bicyclobutane | | | |
|---|---|---|---|---|---|---|---|---|---|---|---|---|---|---|
| $d_2$, cm$^{-1}$ | 1 | 2 | 3 | 4 | 5 | 6 | 7 | 8 | 9 | $d_2$, cm$^{-1}$ | 10 | 11 | 12 | 13 |
| 3138 | 0.996 | −0.089 | −0.012 | 0.000 | 0.000 | 0.001 | 0.000 | 0.000 | 0.000 | 1114 | 0.992 | 0.146 | −0.229 | −0.111 |
| 2274 | 0.120 | 1.310 | −0.231 | 0.003 | 0.020 | 0.034 | −0.005 | −0.003 | −0.004 | 896 | −0.052 | 0.762 | 0.523 | −0.540 |
| 2142 | 0.042 | 0.250 | 1.345 | 0.052 | −0.032 | 0.014 | −0.015 | −0.002 | 0.001 | 815 | −0.368 | 0.946 | −0.676 | 0.260 |
| 1314 | 0.005 | 0.024 | 0.212 | −0.823 | 0.634 | −0.164 | 0.004 | −0.006 | −0.003 | 653 | −0.429 | −0.453 | −0.755 | −0.970 |
| 1059 | −0.015 | −0.143 | −0.030 | 0.860 | 0.871 | 0.208 | −0.183 | −0.039 | −0.017 | | | | | |
| 919 | 0.026 | 0.224 | −0.027 | 0.457 | 0.036 | −1.110 | −0.073 | 0.090 | 0.042 | | | | | |
| 809 | 0.006 | 0.047 | 0.118 | 0.322 | 0.254 | −0.055 | 1.055 | −0.079 | −0.022 | | | | | |
| 631 | −0.002 | −0.002 | 0.040 | 0.027 | 0.119 | 0.193 | 0.111 | 1.013 | −0.113 | | | | | |
| 357 | 0.006 | 0.110 | −0.024 | 0.010 | 0.190 | 0.341 | 0.125 | 0.271 | 1.172 | | | | | |

| $B_1$ block | normal modes of bicyclobutane | | | | | $B_2$ block | normal modes of bicyclobutane | | | | | |
|---|---|---|---|---|---|---|---|---|---|---|---|---|
| $d_2$, cm$^{-1}$ | 14 | 15 | 16 | 17 | 18 | $d_2$, cm$^{-1}$ | 19 | 20 | 21 | 21 | 23 | 24 |
| 3133 | 1.000 | 0.000 | 0.000 | 0.000 | 0.000 | 2274 | 1.330 | 0.145 | −0.018 | −0.018 | −0.019 | 0.008 |
| 1052 | −0.001 | −0.907 | 0.082 | 0.467 | 0.096 | 2156 | −0.154 | 1.362 | 0.041 | 0.033 | −0.026 | −0.006 |
| 915 | 0.002 | 0.518 | −0.070 | 0.885 | −0.296 | 1288 | 0.112 | −0.185 | 0.679 | 0.780 | −0.079 | 0.021 |
| 842 | −0.004 | 0.142 | 1.295 | 0.026 | 0.013 | 1079 | −0.020 | −0.100 | 0.907 | −0.624 | −0.423 | −0.262 |
| 606 | 0.003 | 0.545 | −0.092 | 0.413 | 1.118 | 964 | 0.076 | 0.109 | 0.705 | −0.341 | 0.845 | 0.354 |
| | | | | | | 748 | −0.152 | −0.046 | 0.040 | −0.171 | −0.667 | 1.083 |

**Table XI.** Infrared Intensity Data

| range, cm$^{-1}$ | slope, km/mol | % error in slope | correl coeff | integrated bands |
|---|---|---|---|---|
| | a. Bicyclobutane | | | |
| 3173–3093 | 3.88 | 0.95 | 0.9998 | $\nu_1$, $\nu_{14}$ |
| 3093–3007 | 30.55 | 0.88 | 0.9998 | $\nu_2$, $\nu_{19}$ |
| 3007–2815 | 83.96 | 1.28 | 0.9996 | $\nu_3$, $\nu_{20}$ |
| 1518–1437 | 0.41 | 0.91 | 0.9996 | $\nu_{21}$ |
| 1339–1202 | 2.72 | 0.54 | 0.9999 | $\nu_5$, $\nu_{22}$ |
| 1202–1037 | 26.27 | 0.80 | 0.9997 | $\nu_{15}$, $\nu_{16}$, $\nu_{23}$ |
| 1035–894 | 4.82 | 0.56 | 0.9998 | $\nu_{17}$, $\nu_{24}$ |
| 892–803 | 0.32 | 3.99 | 0.9947 | $\nu_7$ |
| 801–674 | 63.77 | 1.20 | 0.9997 | $\nu_{18}$ |
| 674–599 | 3.09 | 1.14 | 0.9997 | $\nu_8$ |
| | b. Bicyclobutane-$d_2$ | | | |
| 3094–3008 | 30.13 | 0.50 | 0.9999 | $\nu_2$, $\nu_{19}$ |
| 3008–2825 | 86.55 | 0.60 | 0.9999 | $\nu_3$, $\nu_{20}$ |
| 2386–2311 | 0.51 | 2.26 | 0.9971 | $\nu_1$, $\nu_{14}$ |
| 1572–1360 | 1.34 | 0.85 | 0.9997 | $\nu_4$, $\nu_{21}$ |
| 1298–1162 | 3.82 | 0.73 | 0.9997 | $\nu_5$, $\nu_{22}$ |
| 1162–1051 | 18.48 | 0.35 | 0.9999 | $\nu_6$, $\nu_{15}$, $\nu_{16}$ |
| 1051–980 | 0.90 | 0.28 | 0.9999 | $\nu_{23}$ |
| 863–768 | 1.83 | 1.01 | 0.9994 | $\nu_7$, $\nu_{17}$ |
| 766–637 | 58.45 | 0.65 | 0.9999 | $\nu_{18}$, $\nu_{24}$ |
| 552–474 | 0.96 | 2.74 | 0.9963 | $\nu_8$ |

Therefore, the signs of the calculated derivatives were given to the observed values. The use of the $\mathbf{L}^{-1}$ matrix derived from the normal coordinate analysis now allowed the atomic polar tensors (i.e., the dipole moment derivatives with respect to the Cartesian coordinates) to be calculated. Since bicyclobutane has a dipole moment and some antisymmetric vibrational modes will cause a rotation of the molecule in order to conserve angular momentum, it was necessary to apply a rotational correction. It was made by using the procedure of Person and Newton.[18] Thus, if the matrix of $\partial\mu/\partial Q$ is designated as $\mathbf{P}_Q$, and the matrix of polar tensors ($\partial\mu/\partial x$, $\partial\mu/\partial y$, $\partial\mu/\partial z$) is designated is $\mathbf{P}_X$, then

$$\mathbf{P}_R = \mathbf{P}_Q\mathbf{L}^{-1}$$

$$\mathbf{P}_X = \mathbf{P}_R\mathbf{B} + \mathbf{P}_\rho\beta$$

where $\mathbf{B}$ is the $3n - 6 \times 3n$ matrix which gives the transformation between the internal and Cartesian coordinates, $\mathbf{P}_\rho$ is the $3 \times 3n$ matrix which gives the rotational correction in terms of the dipole moment and the moments of inertia, and $\beta$ is the extension to $\mathbf{B}$ which includes the Eckhart conditions for translation and rotation. The values thus derived are given in Table XIII.

If the intensities of overlapping bands have been separated satisfactorily, and the normal coordinates for the parent and its isotopically labeled derivatives have been correctly derived, the atomic polar tensors for the two molecules should be the same. An examination of Table XIII shows that this is the case for bicyclobutane. The deviations were small in all cases, and the agreement in most cases was remarkably good. The theoretically derived atomic polar tensors are in reasonable agreement with

(18) Person, W. B.; Newton, J. H. *J. Chem. Phys.* **1974**, *61*, 1040.

**Table XII.** Observed Intensities[a] and Observed and Calculated Dipole Moment Derivatives[b] in Normal Coordinates for Bicyclobutane

| mode | | $d_0$ obsd int | $d_0$ obsd $\lvert\partial\mu/\partial Q\rvert$ | $d_0$ calcd $\partial\mu/\partial Q$ | $d_2$ obsd int | $d_2$ obsd $\lvert\partial\mu/\partial Q\rvert$ | $d_2$ calcd $\partial\mu/\partial Q$ |
|---|---|---|---|---|---|---|---|
| $A_1$ | 1 | 1.25 | 0.17 | −0.30 | 0.17 | 0.06 | −0.14 |
| | 2 | 18.15 | 0.66 | −0.89 | 18.24 | 0.66 | −0.92 |
| | 3 | 46.28 | 1.05 | 1.22 | 47.52 | 1.06 | 1.21 |
| | 4 | [0.01][c] | | 0.02 | [0.01][c] | | 0.01 |
| | 5 | 1.25 | 0.17 | −0.17 | 1.91 | 0.21 | −0.19 |
| | 6 | [0.01][c] | | 0.01 | 0.14 | 0.06 | 0.05 |
| | 7 | 0.32 | 0.09 | −0.11 | 1.46 | 0.19 | −0.22 |
| | 8 | 3.09 | 0.27 | −0.46 | 0.96 | 0.15 | −0.27 |
| | 9 | [1.01][d] | | 0.15 | [1.6][d] | | 0.20 |
| $B_1$ | 14 | 2.63 | 0.25 | −0.44 | 0.33 | 0.09 | −0.20 |
| | 15 | 18.50 | 0.66 | −0.58 | 17.76 | 0.65 | −0.52 |
| | 16 | 1.20 | 0.17 | −0.24 | 0.58 | 0.12 | 0.09 |
| | 17 | 4.24 | 0.32 | 0.33 | 0.37 | 0.09 | −0.14 |
| | 18 | 63.77 | 1.23 | −1.36 | 58.22 | 1.17 | −1.32 |
| $B_2$ | 19 | 12.39 | 0.54 | 0.73 | 11.88 | 0.53 | −0.74 |
| | 20 | 37.68 | 0.94 | 1.10 | 39.02 | 0.96 | 1.10 |
| | 21 | 0.41 | 0.10 | 0.16 | 1.34 | 0.18 | 0.16 |
| | 22 | 1.47 | 0.19 | −0.19 | 1.91 | 0.21 | 0.19 |
| | 23 | 0.30 | 0.08 | 0.14 | 0.90 | 0.15 | −0.17 |
| | 24 | 0.58 | 0.12 | −0.15 | 0.22 | 0.07 | −0.10 |

[a] Units are km/mol. The uncertainty in the observed intensities is estimated at ±10%. [b] Units are D/(Å amu$^{1/2}$). [c] This band was not observed in the infrared spectrum and was given the small value 0.01. [d] This band was in a region of the spectrum that was noisy and would not give satisfactory integrations. The bands were given the calculated intensities.

the experimental values. Much larger basis sets are required in order to obtain substantially better agreement between calculated and observed values.

The intensities for bicyclobutane-$d_0$ and -$d_2$ were calculated by using the average polar tensors and are compared with the experimental data in Table XIV. This represents a severe test of the derived quantities since the calculated intensities combine errors in the force field and the polar tensors and then square the result. It can be seen that there is rather good agreement, except for $\nu_{16}$. The deviation in this case may be due to an error in the form of the normal coordinate for this vibration, or to an error in the polar tensors caused by an incorrect sign assignment for one of the experimental $\partial\mu/\partial Q$. It is difficult to evaluate these possibilities, but this question will not affect any of the conclusions to be drawn from the results.

It is usually more convenient to use dipole moment derivatives with respect to symmetry coordinates in comparisons among molecules. Therefore, the atomic polar tensors were converted into these derivatives (Table XV). As noted above, an antisymmetric vibration will frequently lead to a rotation of the molecule in order to conserve angular momentum. Therefore, the problem with this transformation is again the need to prevent a rotation of the molecule so as to avoid a contribution from a rotation of the permanent dipole.[19] The transformation was effected by the $\mathbf{B}^{-1}$ matrix which was formed as follows. The $3n - 6 \times 3n$ **B** matrix obtained by using the symmetry coordinates was augmented by using the Eckart conditions to give a $3n \times 3n$ matrix. In constructing the matrix elements corresponding to the Eckart conditions, the masses of two of the carbons were set to a large number (12000) so that a rotation would not occur.[19] For the $B_1$ block, the bridgehead carbons were given a large mass and for the $B_2$ block the methylene carbons were given a large mass. The $\mathbf{B}^{-1}$ matrix was then formed by inversion of **B** in the usual fashion.

Figure 6 shows the symmetry coordinates in diagrammatic form along with the dipole moment derivatives (D/Å). There are some interesting aspects to these data. The largest $\partial\mu/\partial S$ was found with $S_{14}$, an antisymmetric C–C stretching mode. The corresponding mode of [1.1.1]propellane also has the largest $\partial\mu/\partial S$

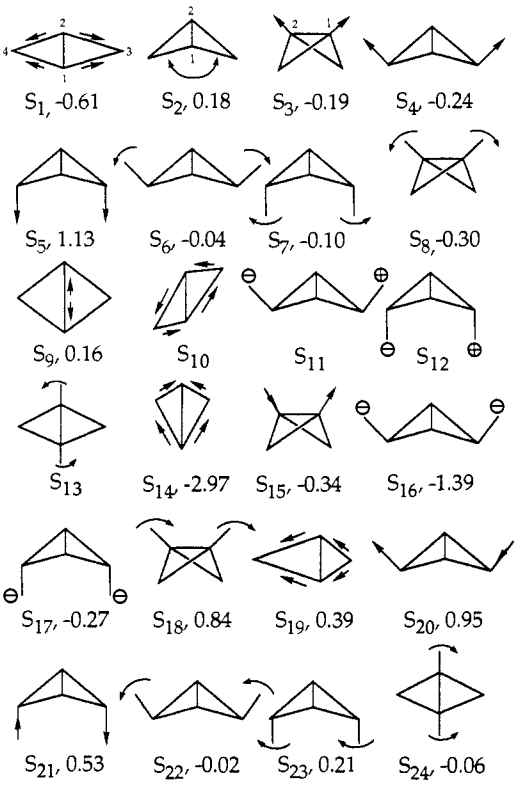


**Figure 6.** Symmetry coordinates and dipole moment derivatives for bicyclo[1.1.0]butane.

(−5.37 D/Å). A change in bond angle at the bridgehead carbons will lead to a change in hybridization, and this in turn will lead to changes in electronegativity and a charge shift.

The symmetric C–H stretching modes $S_3$, $S_4$, and $S_5$ have quite different values of $\partial\mu/\partial S$. We have found that in general the sign of the dipole moment derivative for stretching modes corresponds to the signs of the M–H bond dipoles.[15] In the present case, they correspond to a C–H bond dipole in the sense $C^+$–$H^-$ as has been found for all C–H bonds except those of acetylene (which also give a reversed sign for the dipole moment derivative). Part of the difference in magnitude of the derivatives results from the difference in orientation of the C–H bonds, leading to partial cancellation of the effect due to a single C–H bond. The latter are easily derived from the geometry and are given in Table XVI. The electron populations at the hydrogens as determined by numerical integration of the charge density within the appropriate volume elements also are given in the Table. It can be seen that the changes in $\partial\mu/\partial S$ parallel the changes in population.

## V. Comparison of Bicyclobutane with Cyclopropane and [1.1.1]Propellane

The main object of this study was to make a comparison between the properties of the methylene groups for the three cyclopropane derivatives. It seems appropriate to begin with a comparison of the structural data. The experimental structures are summarized in Table XVII. As is often the case, there is some difficulty in the comparison of these data since the structural parameters were obtained with different experimental techniques (cyclopropane via rotational Raman spectroscopy,[20] bicyclobutane by microwave spectroscopy,[8] and [1.1.1]propellane via electron diffraction[21]). It is well recognized that rotational spectroscopy and electron diffraction lead to different averaging over anharmonic vibrations and lead to different bond lengths for a given molecule.[22] This may, for example, be a component of the

(19) Van Straten, A. J.; Smit, W. M. A. *J. Mol. Spectrosc.* **1975**, *56*, 484.

(20) Butcher, R. J.; Jones, W. J. *J. Mol. Spectrosc.* **1973**, *47*, 64.

(21) Hedberg, L.; Hedberg, K. *J. Am. Chem. Soc.* **1985**, *107*, 7257. Cf. ref 1.

(22) Schwendeman, R. H. *Critical Evaluation of Chemical and Physical Structural Information*; Lide, D. R., Paul, M. A., Eds.; National Academy of Sciences: Washington, DC, 1974; p 94.

**Table XIII.** Observed Atomic Polar Tensors (D/Å) for Bicyclobutane and Bicyclobutane-$d_2$

| | bicyclobutane | | | bicyclobutane-$d_2$ | | | average | | | calculated | | |
|---|---|---|---|---|---|---|---|---|---|---|---|---|
| | $x$ | $y$ | $z$ | $x$ | $y$ | $z$ | $x$ | $y$ | $z$ | $x$ | $y$ | $z$ |
| 1$x$ | −1.49 | 0.00 | 0.03 | −1.47 | 0.00 | 0.00 | −1.48 ± 0.01 | 0.00 | 0.02 ± 0.02 | −1.66 | 0.00 | 0.20 |
| 1$y$ | 0.00 | 0.31 | 0.00 | 0.00 | 0.34 | 0.00 | 0.00 | 0.33 ± 0.02 | 0.00 | 0.00 | 0.34 | 0.00 |
| 1$z$ | 0.19 | 0.00 | −0.39 | 0.15 | 0.00 | −0.41 | 0.17 ± 0.02 | 0.00 | −0.40 ± 0.01 | −0.12 | 0.00 | −0.46 |
| 3$x$ | 0.43 | 0.00 | 0.00 | 0.26 | 0.00 | 0.00 | 0.35 ± 0.09 | 0.00 | 0.00 | 0.62 | 0.00 | 0.00 |
| 3$y$ | 0.00 | 0.49 | −0.04 | 0.00 | 0.51 | −0.22 | 0.00 | 0.50 ± 0.01 | −0.13 ± 0.09 | 0.00 | 0.62 | −0.10 |
| 3$z$ | 0.00 | −0.08 | 1.23 | 0.00 | 0.00 | 1.25 | 0.00 | −0.04 ± 0.04 | 1.24 ± 0.01 | 0.00 | −0.11 | 1.50 |
| 5$x$ | 0.26 | 0.00 | −0.22 | 0.31 | 0.00 | −0.25 | 0.29 ± 0.03 | 0.00 | −0.24 ± 0.02 | 0.13 | 0.00 | −0.35 |
| 5$y$ | 0.00 | −0.07 | 0.00 | 0.00 | −0.05 | 0.00 | 0.00 | −0.06 ± 0.01 | 0.00 | 0.00 | −0.05 | 0.00 |
| 5$z$ | −0.52 | 0.00 | 0.01 | −0.54 | 0.00 | 0.02 | −0.53 ± 0.01 | 0.00 | 0.02 ± 0.01 | −0.68 | 0.00 | 0.03 |
| 7$x$ | 0.73 | 0.00 | 0.00 | 0.71 | 0.00 | 0.00 | 0.72 ± 0.01 | 0.00 | 0.00 | 0.72 | 0.00 | 0.00 |
| 7$y$ | 0.00 | −0.58 | −0.16 | 0.00 | −0.59 | −0.16 | 0.00 | −0.56 ± 0.01 | −0.16 ± 0.01 | 0.00 | −0.68 | −0.19 |
| 7$z$ | 0.00 | −0.34 | −0.06 | 0.00 | −0.33 | −0.05 | 0.00 | −0.34 ± 0.01 | −0.06 ± 0.01 | 0.00 | −0.39 | −0.10 |
| 8$x$ | 0.06 | 0.00 | 0.00 | 0.19 | 0.00 | 0.00 | 0.13 ± 0.07 | 0.00 | 0.00 | 0.19 | 0.00 | 0.00 |
| 8$y$ | 0.00 | −0.15 | −0.04 | 0.00 | −0.22 | −0.05 | 0.00 | −0.19 ± 0.04 | −0.05 ± 0.01 | 0.00 | −0.23 | 0.00 |
| 8$z$ | 0.00 | 0.36 | −0.80 | 0.00 | 0.37 | −0.80 | 0.00 | 0.37 ± 0.01 | −0.80 ± 0.01 | 0.00 | 0.48 | −0.98 |

**Table XIV.** Observed and Calculated Intensities for Bicyclobutane with Averaged Polar Tensors (km/mol)

| mode | | $d_0$ | | $d_2$ | |
|---|---|---|---|---|---|
| | | obsd | calcd | obsd | calcd |
| $A_1$ | 1 | 1.25 | 1.40 | 0.17 | 0.15 |
| | 2 | 18.15 | 17.79 | 18.24 | 18.55 |
| | 3 | 46.28 | 47.05 | 47.52 | 46.78 |
| | 4 | [0.01] | 0.02 | [1.01] | 0.01 |
| | 5 | 1.25 | 1.53 | 1.91 | 1.60 |
| | 6 | [0.01] | 0.08 | 0.14 | 0.04 |
| | 7 | 0.32 | 0.43 | 1.46 | 1.18 |
| | 8 | 3.09 | 3.71 | 0.96 | 0.72 |
| | 9 | [1.01] | 0.93 | [1.6] | 1.58 |
| $B_1$ | 14 | 2.63 | 2.35 | 0.33 | 0.43 |
| | 15 | 18.50 | 19.50 | 17.76 | 15.82 |
| | 16 | 1.20 | 3.27 | 0.58 | 0.01 |
| | 17 | 4.24 | 5.21 | 0.37 | 0.81 |
| | 18 | 63.77 | 61.14 | 58.22 | 59.12 |
| $B_2$ | 19 | 12.39 | 12.13 | 11.88 | 12.14 |
| | 20 | 37.68 | 38.35 | 39.02 | 38.34 |
| | 21 | 0.41 | 0.78 | 1.34 | 0.85 |
| | 22 | 1.47 | 1.67 | 1.91 | 1.56 |
| | 23 | 0.30 | 0.55 | 0.90 | 0.66 |
| | 24 | 0.58 | 0.50 | 0.22 | 0.31 |

**Table XV.** Dipole Moment Derivatives in Symmetry Coordinates (D/Å) for Bicyclobutane

| | calcd | obsd | | |
|---|---|---|---|---|
| | 6-31G* | bicyclobutane | bicyclobutane-$d_2$ | average |
| $S_1$ | −0.60 | −0.52 | −0.69 | −0.61 ± 0.08 |
| $S_2$ | 0.22 | 0.24 | 0.12 | 0.18 ± 0.06 |
| $S_3$ | −0.29 | −0.17 | −0.20 | −0.19 ± 0.02 |
| $S_4$ | −0.31 | −0.24 | −0.24 | −0.24 ± 0.00 |
| $S_5$ | 1.37 | 1.12 | 1.13 | 1.13 ± 0.01 |
| $S_6$ | −0.01 | −0.03 | −0.04 | −0.04 ± 0.01 |
| $S_7$ | −0.12 | −0.09 | −0.11 | −0.10 ± 0.01 |
| $S_8$ | −0.44 | −0.27 | −0.32 | −0.30 ± 0.02 |
| $S_9$ | 0.23 | 0.19 | 0.12 | 0.16 ± 0.04 |
| $S_{14}$ | −3.71 | −3.00 | −2.94 | −2.97 ± 0.03 |
| $S_{15}$ | −0.60 | −0.35 | −0.33 | −0.34 ± 0.01 |
| $S_{16}$ | −1.41 | −1.42 | −1.36 | −1.39 ± 0.03 |
| $S_{17}$ | −0.35 | −0.12 | −0.41 | −0.27 ± 0.14 |
| $S_{18}$ | 0.83 | 0.80 | 0.89 | 0.84 ± 0.05 |
| $S_{19}$ | 0.42 | 0.34 | 0.45 | 0.39 ± 0.06 |
| $S_{20}$ | 1.11 | 0.95 | 0.94 | 0.95 ± 0.01 |
| $S_{21}$ | 0.70 | 0.52 | 0.55 | 0.53 ± 0.02 |
| $S_{22}$ | −0.01 | −0.03 | 0.00 | −0.02 ± 0.01 |
| $S_{23}$ | 0.24 | 0.17 | 0.25 | 0.21 ± 0.04 |
| $S_{24}$ | −0.06 | −0.07 | −0.05 | −0.06 ± 0.01 |

difference in C–H bond lengths between bicyclobutane and [1.1.1]propellane.

It has been found that structures calculated at the MP2/6-31G* level generally agree remarkably well with experimental structures.[23] Therefore, the structures of the compounds of interest

**Table XVI.** Dipole Moment Derivatives for Symmetrical C–H Stretching Modes

| CH bond | $\partial\mu/\partial R$ | population |
|---|---|---|
| bridgehead | 0.15 | 1.009 |
| *exo*-methylene | 0.25 | 1.055 |
| *endo*-methylene | 0.57 | 1.062 |

**Table XVII.** Comparison of Structural Parameters for Methylene Groups

| | propane | cyclo-propane | bicyclo-butane | [1.1.1]-propellane |
|---|---|---|---|---|
| | | a. Observed | | |
| $r$(CH), Å | 1.092 | 1.083 | 1.093 | 1.106 |
| $r$(CC), Å | 1.526 | 1.512 | 1.498 | 1.525 |
| ∠HCH, deg | 106 | 114 | 115.6 | 116 |
| ∠CCC, deg | 112.7 | 60.0 | 60.0 | 63.1 |
| | | b. Calculated, MP2/6-31G* | | |
| $r$(CH), Å | 1.096 | 1.084 | 1.088, 1.092 | 1.088 |
| $r$(CC), Å | 1.525 | 1.502 | 1.492 | 1.514 |
| ∠HCH, deg | 106.3 | 114.2 | 114.1 | 114.2 |
| ∠CCC, deg | 112.4 | 60.0 | 60.2 | 63.5 |

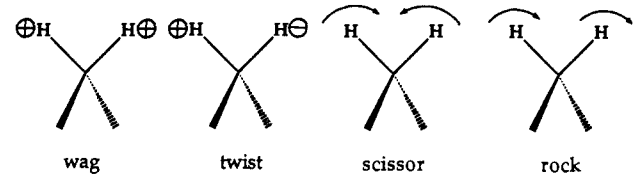


**Figure 7.** Definition of the methylene deformation modes.

were calculated in this fashion, giving the parameters listed in Table XVII. Either set of data indicates that the structures of the methylene groups of the cyclopropane derivatives are very similar, and significantly different than that for propane.

We have taken the experimental data for cyclopropane given by Duncan et al.[24] and have derived force constants[25] in the same fashion as for bicyclobutane and [1.1.1]propellane. However, there is one problem in comparing cyclopropane and propellane with bicyclobutane. The former have methylene groups with local $C_{2v}$ symmetry, leading to a common description of the C–C–H bending symmetry coordinates in terms of scissor, rock, wag, and twist motions (Figure 7). However, bicyclobutane does not have this symmetry. It is however possible to represent it by using corresponding symmetry coordinates (Figure 8), and the normal modes

(23) DeFrees, D. J.; Krishnan, R.; Schlegel, H. B.; Pople, J. A. *J. Am. Chem. Soc.* **1982**, *104*, 5576.

(24) Duncan, J. L.; Burns, G. R. *J. Mol. Spectrosc.* **1969**, *30*, 253.

(25) The force constants for cyclopropane have been derived starting with a 4-31G derived force field (Blom, C. E.; Altona, C. *Mol. Phys.* **1976**, *5*, 1377). For consistency, we have repeated the calculation using the 6-31G* basis set. The two sets of force constants are in very good agreement.

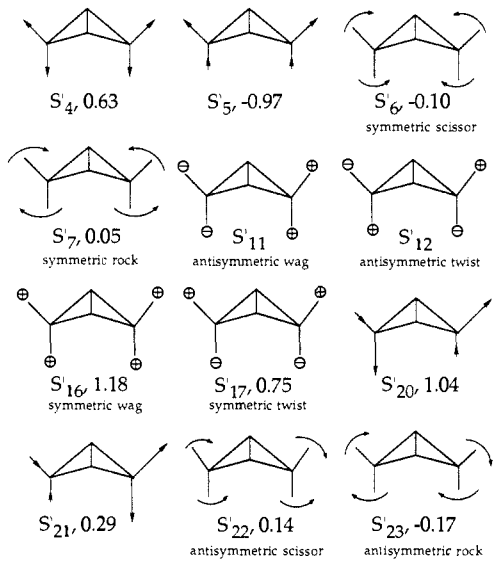


**Figure 8.** Alternate symmetry coordinates and dipole moment derivatives for bicyclo[1.1.0]butane.

**Table XVIII.** Comparison of Force Constant for Cyclopropane, Bicyclobutane, and [1.1.1]Propellane

| mode | propane | cyclo-propane | bicyclo-propane | [1.1.1]-propellane |
|---|---|---|---|---|
| a. Methylene Bending Modes | | | | |
| sym scissor | 0.60 | 1.02 | 1.04 | 0.72 |
| antisym scissor | | 0.99 | 1.05 | 1.06 |
| sym rock | 0.78 | 0.36 | 0.38 | 0.37 |
| antisym rock | | 0.32 | 0.40 | 0.43 |
| sym wag | 0.65 | 0.86 | 1.05 | 1.04 |
| antisym wag | | 1.05 | 1.10 | 0.92 |
| sym twist | 0.63 | 1.40 | 1.10 | 0.82 |
| antisym twist | | 0.87 | 1.05 | 1.00 |
| b. Methylene CH Stretching Modes | | | | |
| sym stretch | 4.79 | 5.25 | 4.95 | 5.20 |
| | | 5.24 | 4.90 | 5.18 |
| antisym stretch | 4.66 | 5.15 | 4.91 | 5.14 |
| | | 5.10 | 5.02 | 5.10 |
| c. C-C Modes | | | | |
| sym stretch | 4.30 | 4.03 | 4.54 | 5.48 |
| antisym stretch | | | 4.14 | 4.01 |
| bridgehead stretch | | | 3.97 | 5.11 |
| flap bend | | | 1.90 | 1.73 |

will take appropriate linear combinations of symmetric and antisymmetric combinations. The data for bicyclobutane also have been analyzed in this fashion, leading to the force constants for the three molecules which are summarized in Table XVIII.[26]

Whereas the four methylene deformation modes of propane have essentially the same force constant, this is not the case with the cyclopropane derivatives. Most of the force constants are larger than those for propane, but for the methylene rock they are markedly smaller. There are some differences in force constants among **1–3**, but there are no major changes. One may ask whether the unusually small force constant for the methylene rocking modes is a consequence of the small bond angle at the methylene, or if it is in some way associated with the special hybridization found with cyclopropane rings. One way in which to obtain information on this question is to examine bicyclo[1.1.1]pentane which has a C–C–C bond angle at the methylene group of only 73.5°.[27] We are in the process of studying this compound.[28]

The C–H stretching force constants for cyclopropane and [1.1.1]propellane are essentially the same, and significantly larger than those for the methylene group of propane. It is interesting that the corresponding force constant for bicyclo[1.1.0]butane has an intermediate value. However, one should not place much emphasis on the C–H stretching force constants since these modes are quite anharmonic, and the difference in apparent force constants could easily arise from differences in anharmonicity. The C–C stretching force constants have no obvious trend, except that it is large for [1.1.1]propellane. It should be noted that a description of cyclopropane ring without the use of redundant coordinates eliminates all of the C–C–C bond angles since they are determined by the bond lengths. Therefore, the stretching of the central bond in [1.1.1]propellane leads to changes in the three C–C–C bond angles as well as the bridgehead C–C–C angles, and this will be reflected in the force constant. Therefore, the large force constant may simply be a result of the cage structure. This question will be further examined when we present data for bicyclo[1.1.1]pentane. The more convenient set of internal coordinates for this molecule includes the 1–3 nonbonded distance and not the C–C–C bond angles. The force constant calculated for the 1,3-interaction will be a measure of the force required to bend the C–C–C bonds.

The dipole moment derivatives also were transformed to the alternate set of symmetry coordinates, and they are shown in Figure 4. As was found with cyclopropane and [1.1.1]propellane, the methylene rock and scissor deformations lead to relatively small dipole moment derivatives. However, in each case, the methylene wag has a large derivative (0.98 for cyclopropane,[2] 1.18 for bicyclobutane, and 1.39 for [1.1.1]propellane[1]). Ethylene also has a large derivative for this deformation (1.37[29]), but for the methylene of propane, it is quite small (0.09[30]).[31] Thus, the large methylene wag derivatives appear to be associated with $sp^2$ hybridized carbons for the methylene groups. The sign of $\partial\mu/\partial S$ shows that when the hydrogens move in the positive coordinate direction, the induced dipole has its positive end in that direction. Thus, it appears that a positively charged hydrogen has moved in the wagging motion. This is contrary to the C–H stretching modes where the sense of the bond dipole was found to be $C^+$–$H^-$. The apparent contradiction results from limited orbital following in this mode, leading to the formation of a bent bond.[14] Here, the proton moves ahead of the overlap charge distribution in the bond leading to an apparent motion of a positively charged atom.

As noted above, the sign of the dipole moment derivatives for the C–H stretching modes corresponds to a bond in the sense $C^+$–$H^-$. There is a general trend toward larger derivatives with greater electron populations at hydrogens, but other factors also are responsible for determining the magnitude of the derivatives. The values for the antisymmetric methylene stretching modes of cyclopropane, bicyclo[1.1.1]butane, and [1.1.1]propellane are all similar (−0.75, −0.97, and −0.44, respectively), although that for the latter is somewhat smaller than for the others.

Despite the apparent similarities among **1–3** with regard to methylene structures, force constants, and dipole moment derivatives, there are some significant differences in other properties. The $^{13}C$ NMR shift tensor normal to the C–C–C plane of the methylene groups varies from −36 ppm for **1** to 41 ppm for **2** and 138 ppm for **3**.[32] This covers nearly the full range of normal $^{13}C$ chemical shifts! Another difference is found in an examination of the topology of the charge distribution for the methylene groups of these molecules. The C–C bond paths were found to curve outwards with cyclopropane (angle between the bond paths at the carbon = 78°), but to be slightly curved inwards for [1.1.1]pro-

(26) The full data are available as supplementary material.
(27) Cox, K. W.; Harmony, M. D. *J. Mol. Spectrosc.* **1970**, *36*, 34.
(28) We have previously reported a normal coordinate analysis for bicyclo[1.1.1]pentane (Wiberg, K. B.; Sturmer, D.; Lewis, T. P.; Levin, I. W. *Spectrochim. Acta* **1975**, *31A*, 57). However, it seems desirable to reexamine it both with regard to checking the vibrational assignment and in order to obtain intensity data.
(29) Golike, R. C.; Mills, I. M.; Person, W. B.; Crawford, B., Jr. *J. Chem. Phys.* **1956**, *25*, 1266.
(30) Kondo, S.; Saëki, S. *Spectrochim. Acta* **1973**, *29A*, 735.
(31) The derivatives are not quite comparable because of the differences in symmetry coordinates. However, the magnitudes are clearly significantly different.
(32) Orendt, A. M.; Facelli, J. C.; Grant, D. M.; Michl, J.; Walker, F. H.; Dailey, W. P.; Waddell, S. T.; Wiberg, K. B.; Schindler, M.; Kutzelnigg, W. *Theor. Chim. Acta* **1985**, *68*, 421.

pellane (bond path angle = 59.4°, conventional angle = 61.8°).[33] The origin of these differences continues to be studied.

**Calculations.** The vibrational frequencies were calculated using GAUSSIAN-86.[34] The transformation of the infrared intensities to atomic polar tensors was carried out using programs written by Dempsey.[35]

**Acknowledgment.** This investigation was supported by a grant from the National Science Foundation.

**Supplementary Material Available:** Tables of alternative symmetry coordinates for bicyclobutane and force constants for bicyclobutane and cyclopropane (4 pages). Ordering information is given on any current masthead page.

(33) Wiberg, K. B.; Bader, R. W. F.; Lau, C. D. H. *J. Am. Chem. Soc.* **1987**, *109*, 985.
(34) Frisch, M. J.; Binkley, J. S.; Schlegel, H. B.; Raghavachari, K.; Melius, C. F.; Martin, R. L.; Stewart, J. J. P.; Bobrowicz, F. W.; Rohlfing, C. M.; Kahn, L. R.; DeFrees, D. J.; Seeger, R.; Whiteside, R. A.; Fox, D. J.; Fleuder, E. M.; Pople, J. A. *Carnegie*-Mellon Quantum Chemistry Publishing Unit, Pittsburgh, PA, 1984.
(35) Dempsey, R. Ph.D. Thesis, Yale University, 1983.

# Reactions of [1.1.1]Propellane

**Kenneth B. Wiberg* and Sherman T. Waddell**

*Contribution from the Department of Chemistry, Yale University, New Haven, Connecticut 06511.*
*Received July 28, 1989*

**Abstract:** The free radical addition reactions of [1.1.1]propellane (**1**) are described in some detail and allowed the preparation of a wide variety of 1,3-disubstituted bicyclo[1.1.1]pentanes. The reaction of **1** with free radicals was more rapid than that of bicyclo[1.1.0]butane (**2**), whereas bicyclo[2.1.0]pentane (**3**) was relatively inert. In some cases the free-radical additions led to oligomers, and in the case of tetrahydrofuran addition the chain-transfer constant was measured. The addition of thiophenol to **1** followed by reduction with the lithium radical anion from 4,4′-di-*tert*-butylbiphenyl gave 1-lithiobicyclo[1.1.1]petane, from which a variety of 1-substituted bicyclo[1.1.1]pentanes may be prepared. In the Baeyer–Villiger oxidation of 1-benzoylbicyclo[1.1.1]pentane, the *tert*-butyl group migrated in preference to the bicyclopentyl group. Conversion of the ketone to the tosylhydrazone followed by base treatment gave products of the type expected from the corresponding carbene. The reaction of **1** with NO in carbon disulfide gave a unique reaction in which nitro and thiocyano groups were introduced. The reactions of **1**, **2**, and **3** with $NO_2$ also were examined. Whereas **1** gave 1,3-dinitrobicyclo[1.1.1]pentane, the other hydrocarbons followed different reaction paths. The reaction of **1** with electron-deficient alkenes and alkynes are described in some detail and are compared with the corresponding reactions of **2** and **3**. Here, the relative reactivities of **1** and **2** were often comparable but varied considerably with the reagent used. Again, **3** was relatively unreactive. The reaction of **1** with Rh(I) gave a dimer, and evidence is presented for a metallocarbene intermediate.

## 1. Introduction

The chemistry of [1.1.1]propellane (**1**) has undergone a remarkable evolution over a relatively short period. It was first predicted to be incapable of existence.[1] It was then theoretically predicted to be readily formed from a 1,3-disubstituted bicyclo[1.1.1]pentane and to be relatively stable, and this was followed by a successful preparation:[2]

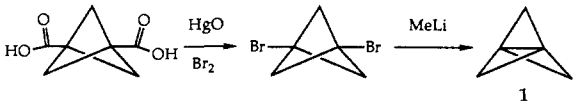


**1**

Subsequently, Szeimies et al. described a remarkably simple preparation for **1**,[3] and it now is one of the most easily obtained of small ring compounds. The ready availability of **1** has made it possible to investigate a wide variety of its reactions which are described herein.

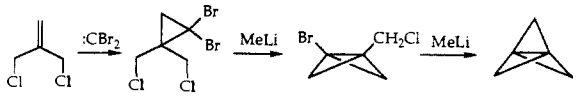


Before examining the reactions of **1**, it may be helpful to compare some of the properties of **1** with those of bicyclo[1.1.0]butane (**2**) and bicyclo[2.1.0]pentane (**3**) (Table I). All three compounds are fairly reactive and will add a variety of substances across the central bond.[1] In addition, each of these compounds has one unique property that may lead to enhanced reactivity.[4]

**Table I.** Properties of Cycloalkanes

| property | 1 | 2 | 3 |
|---|---|---|---|
| ionization potential (eV) | 9.7 | 9.3 | 9.6 |
| strain energy relief (kcal/mol) | 30 | 37 | 49 |
| local charge concn ($-\nabla^2\rho$, e/au$^5$) | 0.33 | 0.23 | 0.19 |

**2** **3**

In those reactions that involve a relatively late transition state, **3** should be the most reactive because fission of its central bond leads to the greatest strain relief.[5] Cleavage of the central bond in **3** eliminates both small rings, whereas with **1** and **2** small rings remain after the cleavage reaction. Another class of reactions, those involving donor–acceptor complexes, have rates of reaction that follow the energy of the highest occupied orbital of the donor.[6] In these cases, the rates are correlated with the ionization potentials, and so **2** should be the most reactive of the three because it has the lowest ionization potential.[7] Finally, all of the com-

(1) Greenberg, A.; Liebman, J. F. *Strained Organic Molecules*; Academic Press: New York, 1978; p 347.
(2) Wiberg, K. B.; Walker, F. H. *J. Am. Chem. Soc.* **1982**, *104*, 5239.
(3) Semmler, K.; Szeimies, G.; Belzner, J. *J. Am. Chem. Soc.* **1985**, *107*, 6410. Belzner, J.; Bunz, U.; Semmler, K.; Szeimies, G.; Opitz, K.; Schlüter, A. *Chem. Ber.* **1989**, *122*, 397.
(4) Wiberg, K. B.; Waddel, S. T.; Laidig, K. E. *Tetrahedron Lett.* **1986**, *27*, 1553.
(5) Wiberg, K. G. *Angew. Chem., Int. Ed. Engl.* **1986**, *25*, 312.
(6) Albright, T. A.; Burdett, J. K.; Whangbo, M. H. *Orbital Interactions in Chemistry*; Wiley: New York, 1985.
(7) Honnegger, E.; Hanspeter, H.; Heilbronner, E.; Dailey, W. P.; Wiberg, K. B. *J. Am. Chem. Soc.* **1985**, *107*, 7172. Bombach, R.; Dannacher, J.; Stadelmann, J.-P.; Neier, R. *Helv. Chim. Acta* **1977**, *60*, 2213. Bieri, G.; Burger, F.; Heilbronner, E.; Maier, J. P. *Helv. Chim. Acta* **1977**, *60*, 2213.

0002-7863/90/1512-2194$02.50/0 